PROCEEDINGS, 49th Workshop on Geothermal Reservoir Engineering
Stanford University, Stanford, California, February 12-14, 2024
SGP-TR-227

Fluid Compositions, Heat Sources and Fracture Interconnectivity in Geothermal Systems Along An Active Subduction Zone

Agnes G. Reyes

GNS-Science 1 Fairway Drive Avalon Lower Hutt, 5101, New Zealand

a.reyes@gns.cri.nz

Keywords: chemistry, subduction fluids, earthquakes, fractures, heat sources

ABSTRACT

It is not common for the forearc of an active subduction zone to have hot springs or localized anomalously high thermal gradients. Among the few in the world are the Nankai subduction zone of Japan, Cascadia in the Pacific Northwest of the USA and the Hikurangi Subduction Zone in eastern North Island in New Zealand where part of the forearc exposed above sea level is referred to as the Subaerial Hikurangi Forearc (SHF). Conductive heating in the SHF is superimposed by heat exothermically generated from regional serpentinization at depth. Increased heat circulation and heat transport in northern SHF, evinced by higher surface conductive heat flow values and the presence of hot springs, is enhanced by (1) a thinner sedimentary cover resulting to a shorter distance between the source of exothermic heat (serpentinizing basalt) and the surface, (2) increased fluid production at depth and (3) higher permeability and faster aqueous fluid ascent rates causing more vigorous fluid circulation (convective rather than conductive). Surface discharge temperatures of the two hot springs in the SHF may be high but subsurface temperatures of pore fluids are similar to that of the cold springs. However, structures in the two hot springs have more direct pathways from depth to surface than in cold springs; and aqueous fluid ascent rates are 23-270x that of cold springs leading to a decrease in heat dissipation. The relative proportion of the four main fluids ascending from depth in the SHF (seawater, water of clay dehydration, water of serpentinization and subducted water) and the mantle gas% in the discharges, whether hot or cold, is associated with the depths of penetration, permeability and interconnectivity at depth of the various structures/faults feeding the surface springs.

1. INTRODUCTION

Conventional geothermal energy sources from hot spring systems are distributed throughout New Zealand although about 99% of surface heat (~4.6 GWt) and 95% of thermal fluids (~120 x 10^6 m^3/a) are discharged in the Taupo Volcanic Zone (TVZ; Bibby et al, 1995; Reyes et al, 2010; Reyes, 2015; Reyes, 2023), the main region of Quaternary volcanism and the prime geothermal power generator in the country. Ngawha in Northland also generates geothermal power but contributes <0.05% of the surface heat and thermal fluid output in New Zealand. Elsewhere of subaerial New Zealand, <1% of the surface heat and <5% of surface thermal fluids are discharged from more than 100 hot spring systems distributed in a wide variety of tectonic settings (Reyes et al, 2010) where surface discharge temperatures are <85°C and estimated subsurface temperatures vary from <100° to ~250°C (Fig. 1A).

One of the tectonic settings for hot springs in New Zealand is located in the exposed forearc (Subaerial Hikurangi Forearc; SHF) of the Hikurangi Subduction Zone in eastern North Island (Fig. 1A) where the Pacific Plate obliquely subducts westward beneath the Australian continental plate (e.g., Davy et al, 2008; Barnes et al, 2018). About 0.0007% of the surface heat (0.029 MWt) and 0.3% of thermal aqueous fluid output (0.38 x 10^6 m^3/a) in subaerial New Zealand are discharged from the SHF. World-wide, it is uncommon for the forearc of an active subduction zone to have hot springs or anomalously high thermal gradients. Among the few known in the world, apart from the HSZ, are located in the forearc of the Nankai subduction zone of Japan including numerous subaerial Arima-type hot springs widely-distributed in the Kii Peninsula with discharge temperatures as high as 93°C (e.g., Kusuda et al, 2014; Umeda et al, 2006; Umam et al, 2022) and anomalously high heat flow measurements (100-250 mW/m^2) offshore (Umeda et al, 2006; Kastner et al, 2014). The advection of hot fluids and high crustal heat flow in the Nankai subduction zone is caused by an unusual and complex concatenation of geological, tectonic and time-dependent factors not found elsewhere (e.g., van Keken and Wilson, 2023). The recently discovered subsea Pythias Oasis in Cascadia in the Pacific Northwest of the USA discharges fluids 9°C higher than the surrounding seawater with an estimated water flux most likely >18 x 10^3 m^3/a, elevated geothermal gradients of 93° to 222°C/km and aqueous fluid expulsion rates of 10-30 cm/sec, values that are unusually very high for the region (Philip et al, 2023).

The objectives of this study are to (1) link seismogenic characteristics and crustal structures with fluid compositions, fluid flowrates, heat distribution and temperatures and (2) explain the anomalous existence of two hot springs and a highly localized area of high heat flow in an active forearc.

2. STUDY AREA

There are more than 500 cold high-Cl springs and CH_4-rich gas vents, some associated with oil seeps and mud volcanoes in the SHF (e.g., McLernon 1978; Francis, 1995; Reyes et al 2022). Surface conductive heat flow increases from <45 mW/m^2 to 62 mW/m^2 (Pandey, 1981; Allis et al, 1998) from south to north. The heat flow values are within the limits of most actively-formed forearcs (e.g., Kastner et al, 2014). The seismogenic zone in the SHF shifts from locked, south of 40.4°S latitude, where slow slip events (SSEs) are generally deeper

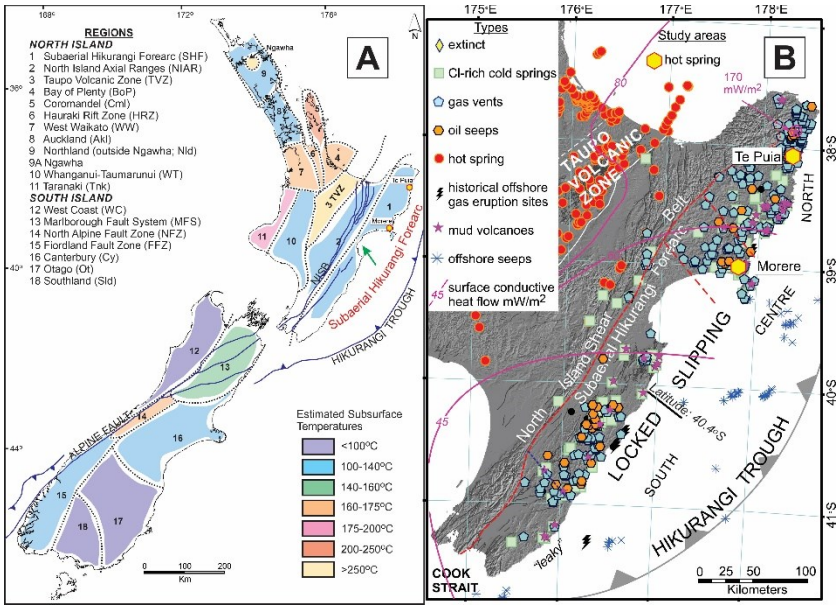

Fig. 1 Maps showing [A] geothermal regions in New Zealand based on tectonic setting showing estimated subsurface temperatures (adapted from Reyes, 2015 and 2018), -location of the two hot springs in the Subaerial Hikurangi Forearc (SHF) and major tectonic features based on Barnes et al (2020), Beanland and Haines (1998), Sutherland et al (2012) and the GNS-Science database; [B] the distribution of fluid vents in the SHF and hot springs in other North Island regions (Reyes et al, 2010; Reyes et al, 2022), general location of the shift in seismogenic regime from locked to slipping (e.g., Wallace, 2020) and conductive surface heat flow iso-contours (Allis et al, 1998).

(>30 km depth), magnitudes greater but frequency of recurrence less (every ~5 years) than in the slipping zone to the north where SSEs occur at depths <15 km over weeks every 1-2 years (e.g., Wallace, 2020). Slow slip events are somewhat like "slow earthquakes" with durations of weeks to months, rather than sudden quick jolts, some with an equivalent M_w as high as 6-7 (e.g., Wallace and Beavan, 2006). The shift from locked to slipping in the forearc of the Hikurangi subduction zone has been hypothesized to be caused by increased fluid saturation and formation overpressures (e.g., Bell et al, 2010; Eberhart-Phillips et al, 2017). This hypothesis was substantiated by field measurements showing that the slipping zone expels 94% of aqueous fluids and 98% of gas with median ascent rates of cold aqueous fluids 3x faster in the slipping zone (Reyes et al, 2022). Fluid vents increase in frequency from south to north in the SHF (Reyes et al, 2022), similar to the distribution offshore (Fig. 1B; Barnes et al, 2010).

The two hot spring systems Morere and Te Puia occur within the slipping zone where the surface conductive heat flow is >50 mW/m^2 (Allis et al, 1998). Te Puia has a maximum discharge temperature of 71ºC and Morere 50ºC and are located where surface conductive heat flow measurements indicate thermal gradients of 30ºC/km and 26ºC/km, respectively. Furthermore, a localized region of anomalously high surface conductive heat flow, also in the slipping zone, reported at 138 mW/m^2 by Pandey (1981) and 170 mW/m^2 by Field et al (1997) occurs in Rotokautuku (Fig. 1B), with an estimated geothermal gradient of 55ºC/km (Pandey, 1981). However, only cold high-Cl springs occur in Rotokautuku.

3. FLOWRATES, STRUCTURES AND AQUEOUS FLUID ASCENT RATES

In general, most of the individual springs with the highest aqueous and gas fluid output are located in the slipping zone. The volume of aqueous fluids discharged in the SHF increases from 3.09 x 10^6 m^3/a in the locked zone to 61.5 x 10^6 m^3/a, a trend also found for gas discharges where 1.8 x 10^7 m^3/a (Normal Temperature and Pressure at 20ºC and 1 bar) is discharged in the locked zone and 79.4 x 10^7 m^3/a (at NTP) in the slipping zone (Figs. 2A and B). In general, the gas:water ratio in cold springs is more than 2x in the slipping than in the locked zone. However, only 0.2% of aqueous fluids expelled in the SHF are hot.

Morere has an estimated flowrate of 9.7 x 10^4 m^3/a of hot aqueous fluids with a gas:water ratio of ~10. Te Puia has a higher hot aqueous fluid flowrate at 28.4 x 10^4 m^3/a but a lower gas:water ratio at 0.1. Cold springs in the high heat flow Rotokautuku region discharge 14 x 10^4 m^3/a aqueous fluids with an estimated gas:water ratio of 0.13. Individual hot spring vents have markedly higher flowrates than cold springs. However, the higher number of vents and the oftentimes much larger area occupied by most cold springs in the SHF result to higher estimates of annual flowrates.

Ascent rates of hot aqueous fluids at Morere is ~25 m/a compared to ~8 m/a at Te Puia, 76x to 24x faster than median ascent rates of cold springs in the slipping zone or 230x to 73x higher than the locked zone cold springs.

Fluid flowrates in the SHF are most copious in fault-associated vents and vents alongside unconformities and stratigraphic contacts. Although nearly all vents in the slipping South and about 10% in the locked zone are associated with active faults, <9% of the total volume of aqueous fluids are released in these regions. In general, NE-SW trending faults in the locked zone and the slipping south (Fig. 2C) are

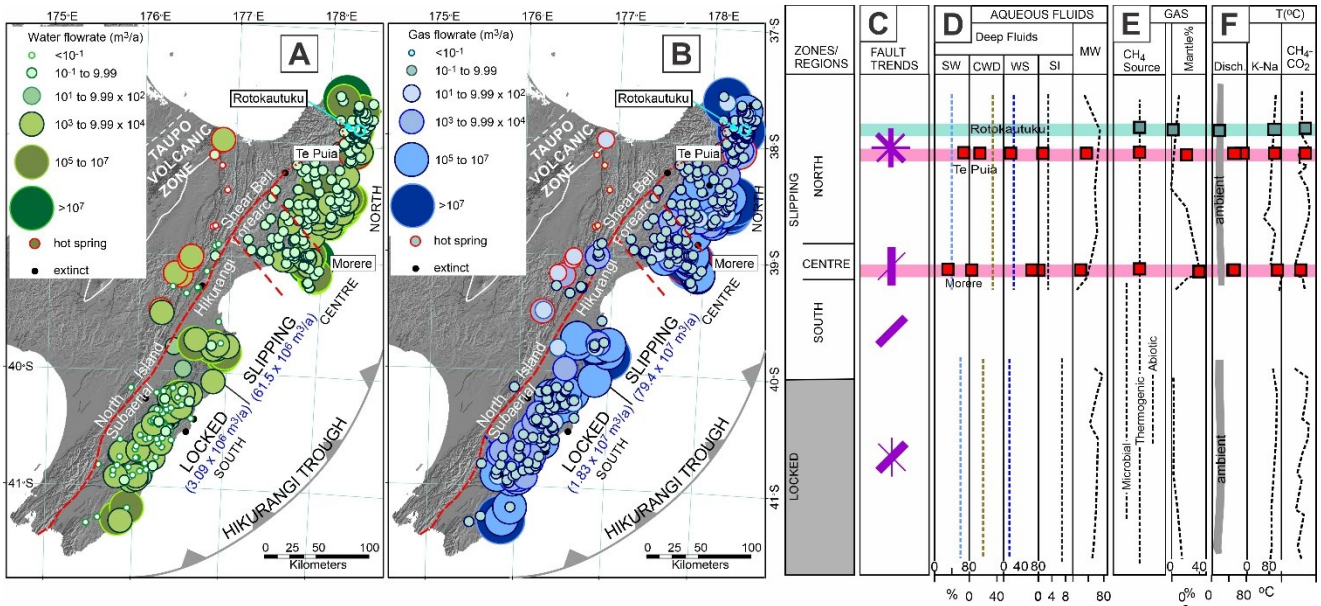

Fig. 2 Maps showing distribution of fluid vents and their [A] water and [B] gas (at NTP: 20ºC, 1 atm.) flow rates (m^3/a). The total water and gas flowrates for the locked and slipping seismogenic zones of the Subaerial Hikurangi Forearc are in blue ink. Seismogenic zones and geographic regions in the SHF are also depicted on the right. [C] Fault trends and the relative volume of aqueous fluids expelled from the faults (the thicker the line, the more copious the volume of expelled aqueous fluids). [D] Relative % of ascending aqueous fluids contributing to the SHF porewaters including SW (seawater), CWD (clay water of dehydration), WS (water of serpentinization) and SI (subducted fluids). The % of meteoric water (MW) input is also shown. [E] Sources of CH_4 gas and the % of mantle-derived gas. [F] Discharge, K-Na and CH_4-CO_2 temperatures. Data from Reyes et al (2022) and Reyes, this study.

the least fluid-productive compared to NS-trending faults in the slipping center. The highest fluid output occurs in the slipping north where numerous cross-cutting faults are prevalent. Interestingly, active faults in the SHF are not necessarily the main fluid conduits.

Mazengarb and Speden (2000) show the Morere hot springs emanating from N-S trending sedimentary beds of an anticline. The Te Puia hot springs and Rotokautuku cold springs occur where variably trending cross-cutting faults are rife (Mazengarb and Speden, 2000), typical of spring occurrences in the slipping North.

In summary, on a regional level, there is a general increase from south to north in the frequency of fluid vents, volume of aqueous and gas fluids and aqueous fluid ascent rates. The two hot springs and a localized high heat flow region occur in the north, within the slipping region, where thermal gradients are higher than in the south. Hot springs have aqueous fluid ascent rates 24-230x that of cold springs.

4. FLUID SOURCES

4.1 Aqueous fluids

As shown in Fig. 2D, ascending fluids in the SHF consist of seawater (SW), clay water of dehydration (CWD), water of serpentinization from hydration of basaltic crust (WS) and subducted aqueous fluids (SI) that have been subjected to prolonged water-rock interaction. Clay water of dehydration is low-Cl water with positive $\delta^{18}O$ values, expelled from progressive transformation of labile clays including smectite, to interlayered clays, and thence to illite or chlorite during diagenesis (e.g., Volker and Stipp, 2015; Reyes et al, 2022). Modeling (Reyes et al, 2022) shows that porewaters in the locked zone contain 60% SW, 7% SI, 20% CWD and 13% WS. Porewaters in the slipping zone have higher proportions of CWD (34%) and WS (23%) but less SW (40%) and SI (3%) than in the locked zone. Compared to the norm in the slipping zone, Morere and Te Puia aqueous fluids contain less CWD. Porewaters expelled in Te Puia also have a slightly less proportion of WS than the norm but has 5x the norm in Morere suggesting that the main avenue for water of serpentinization to the surface is at and around Morere. Meteoric water (MW) influx is late-stage, introduced after uplift of the forearc, and continues to this day. The proportion of MW input varies from 10-77% with the main hot springs at Morere having 20% and Te Puia, 35%.

4.2 Gas

Methane is the main gas expelled in the SHF. The source of CH_4 is based on $\delta D(CH_4)$ and $\delta^{13}C(CH_4)$ isotopic compositions. Most CH_4 expelled in the SHF is thermogenic (Fig. 2E), suggesting diagenetic temperatures of at least 75°C (Clayton, 1991), with some biogenic occurrences in the locked zone and abiotic CH_4, derived from serpentinization (Milkov and Etiope, 2018), occurring in the locked zone and the slipping south. The % of mantle gas, based on the ratio of $^3He/^4He$ of the sample to that of air (R/Ra) and assuming R/Ra= 8.0 for 100% mantle gas (e.g., Ozima and Podosek, 2002), varies from <5% (crustal) to a high of 42% in the slipping center. Mantle gas is elevated in Morere and Te Puia at 42% and 24%, respectively compared to crustal for Rotokautuku at 4%.

5. TEMPERATURES

Subsurface temperatures are estimated for clay water of dehydration (CWD) and water of serpentinization (WS), the two main fluid end-members generated within the rock formations in the SHF, using isotopic compositions and fractionation factors (Reyes et al, 2022). CWD is generated over a wide range of temperatures at <65°C to 185° ± 25°C at depths <3 km to >12 km whilst WS is generated at >185° + 25°C at depths >12 km. Thermogenic gas is generated at >75°C (Clayton, 1991) and abiotic CH_4, possibly at >150°C in the SHF. Porewaters are a combination of SW, CWD, WS, and SI, as described in Section 4.1 with dissolved gas composed mostly of CH_4 and are the main and most copious fluids discharges throughout the SHF, relative to individual end-member fluids.

A high proportion of porewater is discharged to the surface at Morere (80%) and Te Puia (65%) with surface discharge temperatures varying with the proportion of meteoric water input. Thus, discharge temperatures in the hot springs range from 45-51°C at Morere and 58-70°C at Te Puia. In general, the median K-Na temperatures of Morere and Te Puia fluids are similar to cold springs but slightly higher for CH_4-CO_2 (Fig. 2F). A more detailed comparison between chemical geothermometric temperatures in the two hot springs, Rotokautuku cold spring in a high heat flux region and other SHF cold springs is shown in Figs. 3A and B, superimposed on the temperature ranges of the main calc-alkaline clays found in most active forearcs.

Median subsurface temperatures vary from 80-110°C for K-Na (Fig. 3A) and 90-120°C for CH_4-CO_2 (Fig. 3B) geothermometry with a clear-cut increase in temperature from south to north for the latter. Although individual K-Na temperatures for Morere and Te Puia hot springs can be higher than the median temperatures across the SHF, only Morere (up to 125°C for several measurements) has K-Na temperatures extending above that of cold springs (range: 60-115°C) but still within the ±25°C slack for subsurface geothermometric estimates. CH_4-CO_2 temperatures in Morere and Te Puia are within the range for cold springs at 60°-135°C, ±25°C.

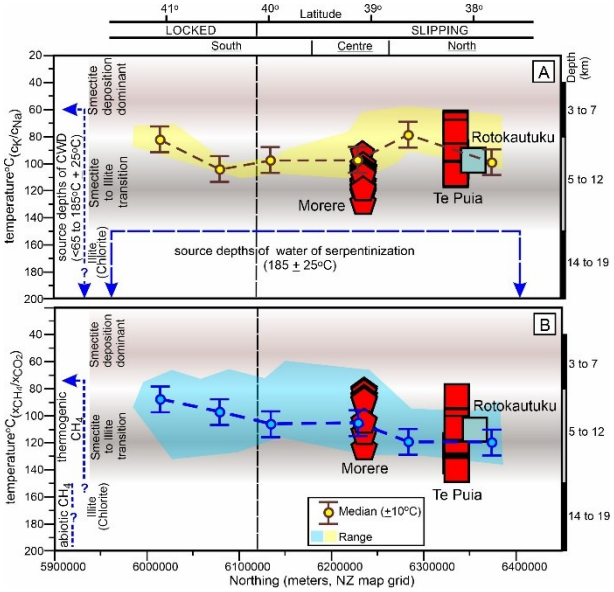

Fig. 3 South to north transect showing the range and median subsurface temperatures of cold springs indicated by [A] K-Na and [B] CH_4-CO_2 geothermometry with data points for Morere and Te Puia hot springs and Rotokautuku cold spring also shown. Clay formation temperatures in the SHF and most forearcs and sedimentary basins, are lower than in high-temperature geothermal systems (e.g., Velde, 1985). Geothermometers are from Giggenbach (1991). Depths are estimated assuming an average geothermal gradient of 11° ± 4°C/km at the interface from various thermal models (e.g., Fagereng and Ellis, 2009) for the Hikurangi margin.

In summary, subsurface temperatures of hot discharges in Morere and Te Puia and cold fluids in the high-heat flow Rotokautuku are similar to that of cold fluids venting in the SHF.

6. GEOCHEMICAL MODEL

There are two types of Cl-rich aqueous fluids in the SHF: Na-Cl and Na-Ca-Cl with the introduction of meteoric water resulting to Na-(Ca)-Cl-HCO_3 compositions (Figs. 4A and B). Na-Cl waters and associated thermogenic gas are generated within the sedimentary rock formations during diagenesis. Serpentinization of basaltic crust (Fig. 4C) expels very high Cl waters (>10,000 mg/kg) and produces Na-Ca-Cl waters with elevated isotopic δD values and abiotic CH_4 (Reyes et al, 2022). Primordial ^3He ascends along deep interconnected faults from the upper mantle to the surface.

The Morere hot springs have some of the highest mantle gas input (42%) and Cl concentrations (16,000 mg/kg Cl) in the SHF with the latter attributed to a high proportion of water of serpentinization. Te Puia hot springs also have relatively high mantle gas and water of serpentinization proportions albeit less than Morere. The high values have led Giggenbach et al (1995) to conclude that serpentinization and high values of mantle gas are genetically related. This may be partly true for Morere where interconnected faults may tap into very

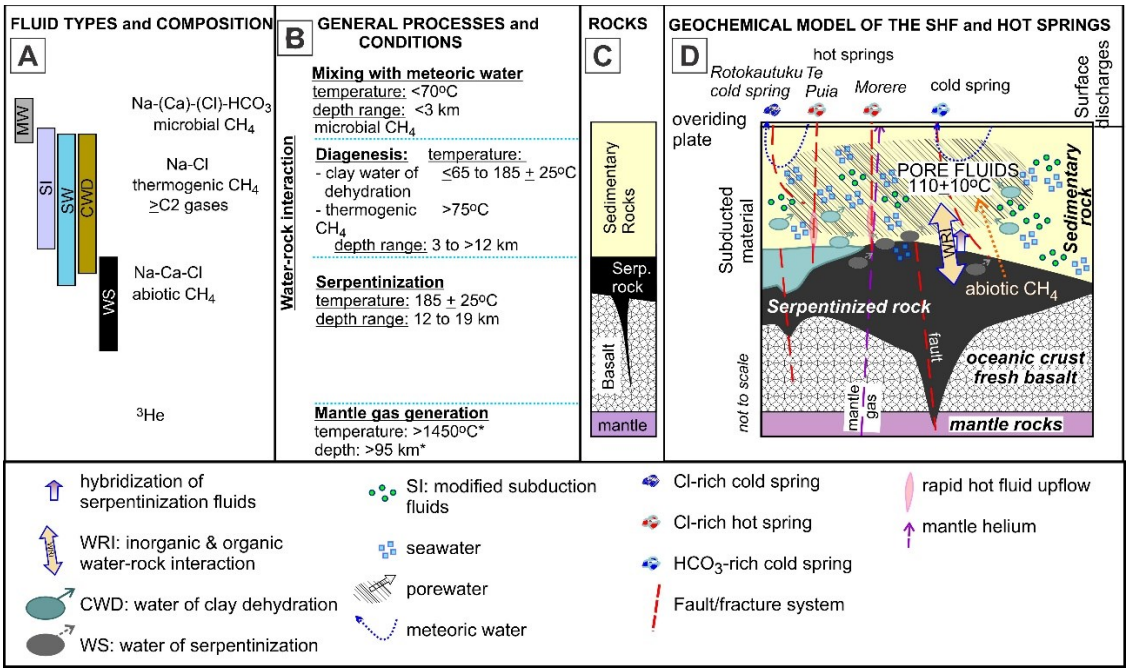

Fig. 4 [A] Fluid types and general chemical compositions. [B] General processes and conditions (temperature and depth) from the surface and the overriding plate to the subducted Pacific plate consisting of sedimentary rocks, basaltic crust with a serpentinization front and the upper mantle. [C] Rocks in the SHF. [D] Cartoon (not to scale) showing the cross-sectional distribution of the different types of fluids and rocks in the SHF and the general composition of surface spring fluids. Straight red broken lines are faults providing direct channels for deep fluids ascending from depth to the surface. Fault tortuosity is depicted by red curved broken lines. Except for the temperature and depth of the upper mantle (Antriasian et al, 2019), the rest of the figure is derived from Reyes et al (2022) and Reyes (unpublished data).

deep structures that extend to the mantle. But other data here and in Reyes et al (2022) show a decoupling of high mantle gas with serpentinization (Fig. 4D).

Variation in the proportions of ascending seawater, subducted water subjected to prolonged water-rock interaction (SI), water of serpentinization and clay water of dehydration is dependent on the depths of crustal penetration, permeability and interconnectivity of the various structures/faults feeding the surface hot and cold springs (Fig. 4D).

6.1. Why are Morere and Te Puia hot?

Pore fluids consisting of aqueous fluids from various sources and dissolved gas, have an estimated temperature of 110 ± 10ºC (Fig. 4D). The Morere and Te Puia hot spring fluids, despite high surface discharge temperatures of 51º and 70ºC, have the same temperatures at depth as the cold vents that proliferate the SHF. The difference in discharge temperatures between the hot springs and the cold vents can be ascribed to a faster rate of ascent of aqueous fluids in the hot springs estimated to be 24x to 270x that of the cold springs. A higher rate of ascent suggests more vigorous fluid circulation which enhances heat transport, rather than conduction alone, and localized higher permeability indicated by higher flowrates in individual hot spring vents than in cold vents. It is suggested here that hot spring structures provide more direct channels from depth to surface with cold vents fed by faults/structures with higher tortuosity. The more direct the pathway to the surface, the less heat dissipates into the surrounding colder rock.

Rotokautuku, a set of cold springs within a region of high heat flow, has similar chemical and isotopic compositions and subsurface temperatures as other cold vent discharges. Previous measurements by Pick (1962) suggest ascent rates and flowrates within the range of other SHF cold spring systems. Geochemically and from field measurements used in this study, the high heat flow at Rotokautuku cannot be explained.

7. SUMMARY AND CONCLUSIONS

As the seismogenic regime shifts from locked in the south to slipping in the north in the Subaerial Hikurangi Forearc, the volume of aqueous fluid discharge increases by ~20% and gas by ~43%, substantiating the hypothesis previously presented by geophysical studies. Higher flowrates in the north are attributed to (1) the occurrence of more permeable N-S striking and numerous cross-cutting faults/structures, as opposed to NE-SW striking structures in the south and (2) more copious generation of fluids in the north. There are four types of aqueous fluids in the SHF ascending from depth including seawater (SW), clay water of dehydration (CWD), water of serpentinization (WS) and subducted fluids subjected to prolonged water-rock interaction (SI) with meteoric water entering the system upon subaerial uplift of the forearc. Water of serpentinization and clay water of dehydration are generated at ≥185º±25ºC at ~12-19 km and from <65 to ~185º+25ºC at <3 to >12 km, respectively. Thermogenic, with less commonly-occurring biogenic and abiotic gases, occur as dissolved species at >75ºC. The various fluids form 110º±10ºC pore fluids, distributed throughout the SHF at depth.

Temperatures at depth in the SHF can be attributed to conductive heating with an estimated thermal gradient of 11°± 4°C/km at the plate interface and the hydration of basalt (serpentinization), an exothermic process. The northwards increase in surface conductive heat flow can be, in part, due to a thinner sedimentary cover (less distance between the heat-generating serpentinized basalt crust from the surface) in the north coupled by higher aqueous flow rates and ascent rates of vents. The higher proportion of water of serpentinization in pore fluids in the north (23%) suggests a higher degree of serpentinization, and hence a higher production of exothermic heat, than in the south where the WS proportion is only 13%.

The proportions of SW, CWD, WS and SI in spring discharges can be attributed to the depths of penetration into the crust, interconnectivity and tortuosity of the various structures associated with each spring system in the SHF.

The anomalous occurrence of hot springs in the SHF can be ascribed to a faster rate of ascent of aqueous fluids estimated at 24x to 270x that of the cold springs. Vigorous fluid circulation enhances heat transport. It is suggested here that hot spring structures provide more direct avenues from depth to surface compared to cold vents fed by faults/structures with higher tortuosity. The more direct the pathway towards the surface, the less the heat dissipation into the surrounding colder rock. The high heat flow at Rotokautuku cannot be explained using the methods in this study.

REFERENCES

Allis, R.G., Funnell, R.H., and Zhan, X.: From Basins to Mountains and Back Again: N.Z. Basin Evolution since 10 Ma, Proceedings, 9th International Symposium on Water-Rock Interaction, Taupo, New Zealand, (1998), 3–9.

Antriasian, A., Harris, R.N., Trehu, A.M., Henrys, S.A., Phrampus, B.J., Lauer, R., Gorman, A.R., Pecher, I.A., and Barker, D.: Thermal Regime of the Northern Hikurangi Margin, New Zealand, Geophys. J. Int., 216, (2019), 1177–1190.

Barnes, P.M., Ghisetti, F.C., Ellis, S., and Morgan, J.K.: The Role of Protothrusts in Frontal Accretion and Accommodation of Plate Convergence, Hikurangi Subduction Margin, New Zealand, Geosphere, 14, (2018), 440–467.

Barnes, P.M., Lamarche, G., Bialas, J., Henrys, S., Pecher, I., Netzeband, G.L., Greinert, J., Mountjoy, J.J., Pedley, K., and Crutchley, G.: Tectonic and Geological Framework for Gas Hydrates and Cold Seeps on the Hikurangi Subduction Margin, New Zealand, Mar. Geol., 272, (2010), 26–48.

Barnes, P.M., Wallace, L.M., Saffer, D.M., Bell, R.E., Underwood, M.B., Fagereng, Å., Meneghini, F., Savage, H.M., and IODP Expedition 372 Scientists: Slow Slip Source Characterized by Lithological and Geometric Heterogeneity, Sci. Adv., 6, (2020).

Beanland, S., and Haines, J.: The Kinematics of Active Deformation in the North Island, New Zealand, Determined from Geological Strain Rates, N.Z.J. Geol. Geophys., 41, (1998), 311–323.

Bell, R., Sutherland, R., Barker, D.H.N., Henrys, S., Bannister, S., Wallace, L., and Beavan, J., 2010. Seismic Reflection Character of the Hikurangi Subduction Interface, New Zealand, in the Region of Repeated Gisborne Slow Slip Events, Geophys. J. Int., 180, (2010), 34- 48.

Bibby, H.M., Caldwell, T.G., Davey, F.J., and Webb, T.H.: Geophysical Evidence on the Structure of the Taupo Volcanic Zone and its Hydrothermal Circulation, J. Volcanol. Geotherm. Res., 68, (1995), 29–58.

Clayton, C.: Carbon Isotope Fractionation During Natural Gas Generation from Kerogen, Mar. Pet. Geol., 8, (1991), 232–240.

Davy, B., Hoernle, K., and Werner, R.: Hikurangi Plateau: Crustal Structure, Rifted Formation, and Gondwana Subduction History, Geochem. Geophys. Geosyst., 9, (2008), 31p

Eberhart-Phillips, D., Bannister, S., and Reyners, M.: Deciphering the 3–D Distribution of Fluid along the Shallow Hikurangi Subduction Zone using P- and S-wave Attenuation, Geophys. J. Int., 211, (2017), 1032–1045.

Fagereng, Å. and Ellis, S.: On Factors Controlling the Depth of Interseismic Coupling on the Hikurangi Subduction Interface, New Zealand, Earth Planet. Sci. Lett., 278, (2009), 120–130.

Field, B.D., Uruski, C.I., Beu, A.G., Browne, G.H., Crampton, J.S., Funnell, R.H., Killops, S.D., Laird, M., Mazengarb, C., Morgans, H.E.G., Rait, G.J., Smale, D., and Strong, C.P., 1997. Cretaceous-Cenozoic Geology and Petroleum Systems of the East Coast Region, New Zealand, Institute of Geological and Nuclear Sciences Monograph, 19, (1997), Lower Hutt, New Zealand.

Francis, D.A.: Oil and Gas Seeps of Northern and Central East Coast Basin, Petrol. Explo. New Zealand News, 44, (1995), 21–27.

Giggenbach, W.F.: Chemical Techniques in Geothermal Exploration, In: D'Amore, F. (Coordinator): Applications of Geochemistry in Geothermal Reservoir Development, UNITAR/UNDP, Rome, Italy, (1991), 119-144.

Giggenbach, W.F., Stewart, M.K., Sano, Y., Goguel, R.L., and Lyon, G.L.: Isotopic and Chemical Composition of Solutions and Gases from the East Coast Accretionary Prism, New Zealand, In: Isotope and Geochemical Techniques Applied to Geothermal Investigations, IAEA-TECDOC 788, (1995), 209–231.

Kastner, M., Solomon, E.A., Harris, R.N., and Torres, M.E.: Fluid Origins, Thermal Regimes, and Fluid and Solute Fluxes in the Forearc of Subduction Zones, Dev. Marine Geol., 7, (2014), 671–733.

Kusuda, C., Iwamori, H., Nakamura, H., Kazahaya, K., and Morikawa, N.: Arima Hot Spring Waters as a Deep-Seated Brine from Subducting Slab, Earth, Planets and Space, 66, (2014), 13p.

Macpherson, E.O.: Te Puia Hot springs, N.Z.J. Sci. and Tech., 26B, (1945), 244-254.

Mazengarb, C. and Speden, I.G.: Geology of the Raukumara Area: 1:250,000 Geological Map 6, (2000), Institute of Geological & Nuclear Sciences, Wellington New Zealand, 60p.

McLernon, C.R.: Indications of Petroleum in New Zealand, Unpublished Petroleum Report 839, (1978), Ministry of Economic Development, Wellington, New Zealand, 607p.

Milkov, A.V. and Etiope, G.: Revised Genetic Diagram for Natural Gases based on a Global Dataset of >20,000 Samples, Org. Geochem., 125, (2018), 109–120.

Ozima, M. and Podosek, F.A.: Noble Gas Geochemistry, Cambridge University Press, U.K., (2002), 302p.

Pandey, O.P.: Terrestrial Heat Flow in New Zealand, PhD thesis, (1981), Victoria University of Wellington, New Zealand, 210p.

Philip, B.T., Solomon, E.A., Kelley, D.S., Tréhu, A.M., Whorley, T.L., Roland, E., Tominaga, M., and Collier, R.W.: Fluid Sources and Overpressures within the Central Cascadia Subduction Zone Revealed by a Warm, High-Flux Seafloor Seep, Sci. Adv., 9, (2023), 13p.

Pick, M.C.: The Stratigraphy, Structure and Economic Geology of the Cretaceo-Tertiary Rocks of the Waiapu District, New Zealand, PhD thesis, University of Bristol, UK, (1962).

Reyes, A.G.: Low-Temperature Geothermal Reserves in New Zealand, Geothermics, 56, (2015), 138-161.

Reyes, A.G.: Geothermal Energy from Abandoned Petroleum Wells in New Zealand, Proceedings, 12th Asian Geothermal Symposium, Daejeon, Korea, (2018).

Reyes, A.G.: Evaluation of Critical Elements in Geothermal Systems of the Taupo Volcanic Zone, New Zealand, Proceedings, 2023 World Geothermal Congress, Beijing, China (2023).

Reyes, A.G., Christenson, B.W., and Faure, K.: Sources of Solutes and Heat in Low-Enthalpy Mineral Waters and Their Relation to Tectonic Setting, New Zealand, J. Volcanol. Geotherm. Res., 192, (2010), 117–141.

Reyes, A.G., Ellis, S.M., Christenson, B.W., and Henrys, S.: Fluid Flowrates and Compositions and Water–Rock Interaction in the Hikurangi Margin Forearc, New Zealand, Chem. Geol., 614, (2022), 29 p.

Sutherland, R., Toy, V.G., Townend, J., Cox, S.C., Eccles, J.D., Faulkner, D.R. and 14 others: Drilling Reveals Fluid Control on Architecture and Rupture of the Alpine Fault, New Zealand, Geology, 40, (2012), 1143-1146.

Umam, R., Tanimizu, M., Nakamura, H., Nishio, Y., Nakai, R., Sugimoto, N., and 6 others: Lithium Isotope Systematics of Arima Hot Spring Waters and Groundwaters in Kii Peninsula, Geochem. J., 56, (2022), e8-e17.

Umeda, K., Kanazawa, S., Kakuta, C., Asamori, K., and Oikawa, T.: Variations in the $^{3}He/^{4}He$ Ratios of Hot Springs on Shikoku Island, Southwest Japan, Geochem. Geophys. Geosyst., 7, (2006), 11p.

Van Keken, P.E. and Wilson, C.R.: An Introductory Review of the Thermal Structure of Subduction Zones: I- Motivation and Selected Examples, Prog. In Earth and Planet. Sci., 10, (2023), 20p.

Velde, B.: Clay Minerals: A Physico-Chemical Explanation of Their Occurrence, Elsevier, (1985), 427p.

Völker, D. and Stipp, M.: Water Input and Water Release from the Subducting Nazca Plate Along Southern Central Chile (33°S–46°S), Geochem. Geophys. Geosyst., 16, (2015), 1825-1847.

Wallace, L.M.: 2020. Slow Slip Events in New Zealand, Annu. Rev. Earth Planet. Sci., 48, (2020), 8.1–8.29.

Wallace, L.M. and Beavan, R.J.: A Large Slow Slip Event on the Central Hikurangi Subduction Interface Beneath the Manawatu region, North Island, New Zealand. Geophys. Res. Lett., 33, (2006), 4p.